View metadata, citation and similar papers at core.ac.uk

brought to you by CORE

provided by Elsevier - Publisher Connector

Neoplasia • Vol. 7, No. 1, January 2005, pp. 7–16

www.neoplasia.com

Gene Expression Profile of Glioblastoma Multiforme Invasive Phenotype Points to New Therapeutic Targets[1]

Dominique B. Hoelzinger[*,†], Luigi Mariani[‡], Joachim Weis[§], Tanja Woyke[¶], Theresa J. Berens*, Wendy S. McDonough*, Andrew Sloan[#], Stephen W. Coons** and Michael E. Berens*

*Translational Genomics Research Institute (TGen), Phoenix, AZ 85004, USA; [†]Arizona State University, Tempe, AZ 85281, USA; [‡]Department of Neurosurgery, University Hospital, Inselspital, Bern CH-3010, Switzerland; [§]Institute of Neuropathology, Universitätsklinikum der RWTH, Aachen D-52074, Germany; [¶]Lawrence Berkeley National Laboratory, Walnut Creek, CA 94598, USA; [#]Departments of Neurosurgery and Integrative Oncology, H. Lee Moffit Cancer Center and Research Institute, Tampa FL, 33612-9497, USA; **Department of Neuropathology, St. Joseph's Hospital, Phoenix, AZ 85013, USA

Abstract

The invasive phenotype of glioblastoma multiforme (GBM) is a hallmark of malignant process, yet molecular mechanisms that dictate this locally invasive behavior remain poorly understood. Gene expression profiles of human glioma cells were assessed from laser capture–microdissected GBM cells collected from paired patient tumor cores and white matter–invading cell populations. Changes in gene expression in invading GBM cells were validated by quantitative reverse transcription polymerase chain reaction (QRT-PCR) and immunohistochemistry in an independent sample set. QRT-PCR confirmed the differential expression in 19 of 21 genes tested. Immunohistochemical analyses of autotaxin (ATX), ephrin B3, B-cell lymphoma-w (BCLW), and protein tyrosine kinase 2 beta showed them to be expressed in invasive glioma cells. The known GBM markers, insulin-like growth factor binding protein 2 and vimentin, were robustly expressed in the tumor core. A glioma invasion tissue microarray confirmed the expression of ATX and BCLW in invasive cells of tumors of various grades. GBM phenotypic and genotypic heterogeneity is well documented. In this study, we show an additional layer of complexity: transcriptional differences between cells of tumor core and invasive cells located in the brain parenchyma. Gene products supporting invasion may be novel targets for manipu

lation of brain tumor behavior with consequences on treatment outcome.

Neoplasia (2005) **7,** 7–16

Keywords: Glioma, invasion, cDNA microarray, expression profile, tissue microarray.

Introduction

Glioblastoma multiforme (GBM) is the most common and most lethal primary malignant brain tumor. These nonmetastatic tumors are highly locally invasive [1], diffusely disseminating into the brain and placing cells outside the margin of therapeutic resection. Current therapies address the bulk of the tumor mass, whereas recurrence is most often within 3 cm of the resection margin [2] and accounts for the fatal outcome of the disease. The infiltrative path of GBM into the normal brain is not random; it often follows white matter tracts and extends along perivascular spaces, the glia limitans externa and the subependyma [3]. Little is known about the distinct biology of invasive glioblastoma cells *in situ*, but their diffuse infiltration suggests the activation of genetic and cellular programs that distinguish them from cells in the tumor core.

Microarray technology has proven to be very useful in the molecular classification of astrocytic tumor grades [4–9], generating evidence of a molecular evolution driving progressive stages of astrocytoma malignancy. Gene expression analysis enhances histopathologic diagnosis [7,8], specifically of nonclassic tumor histologies, providing a more accurate prognosis [4,10]. It is hoped that molecular characterization of tumor subtypes will lead to the application of therapy customized to a particular tumor's biology. This report illustrates the usage of cDNA microarrays to discern differential gene expression comparing glioma cells at a stationary, proliferative site within the tumor core to cells invading the surrounding brain exhibiting a diffuse, motile behavior. Patterns of gene expression by cells at the tumor core, such as the presence of insulin-like growth factor binding protein 2 (*IGFBP2*), were consistent with published cDNA microarray characterizations of GBM [5,6,9]. Genes upregulated in invasive cells depict a commitment to motility and invasion, such as the autocrine motility factor, autotaxin (*ATX*), and protein tyrosine kinase 2 beta (*PYK2*). Increased expression of the antiapoptotic *BCLW* and death-associated protein 3 (*DAP3*), a protein previously found to be

Abbreviations: GBM, glioblastoma multiforme; LCM, laser capture microdissection; TMA, tissue microarray

Address all correspondence to: Michael E. Berens, 400 North Fifth Street, Suite 1600, Phoenix, AZ 85004. E-mail: mberens@tgen.org

[1]This work was supported by NIH-NS 42262.

Received 6 August 2004; Revised 22 September 2004; Accepted 28 September 2004.

Copyright © 2005 Neoplasia Press, Inc. All rights reserved 1522-8002/05/$25.00

DOI 10.1593/neo.04535

Table 1. Genes Downregulated in Invasive GBM.

I/C	Accession Number	Number	Description
Extracellular			
0.16	N91385	MS4A1	Membrane-spanning 4-domains, A1
0.2	AA429895	ABCC3	ATP-binding cassette C (CFTR/MRP)
0.25	AA448569	SRPX	Sushi repeat–containing protein, X chromosome
0.25	AA598653	OSF2	Osteoblast-specific factor 2 (fasciclin 1–like)
0.33	N76878	DEPP	Decidual protein induced by progesterone
0.33	T77595	TNC	Tenascin C (hexabrachion)
0.33	H79047	IGFBP2	Insulin-like growth factor binding protein 2
0.33	R7563.5	COLA1	Collagen, type V, alpha 1
0.33	T49159	SERPIN	Serine (or cysteine) proteinase inhibitor, clade B 2
0.5	R71440	SERPINH2	Serine (or cysteine) proteinase inhibitor, clade H2 (hsp47)
0.5	M65062	IGFBP5	Insulin-like growth factor binding protein 5
Vascular involvement/angiogenesis			
0.25	AA029842	MTCP1	Mature T-cell proliferation 1
0.25	AA401693	CD163	CD163
0.33	H16637	VCAM1	Vascular cell adhesion molecule 1
0.33	AA421296	CD68	CD68 antigen
0.33	A4491191	IF116	Interferon gamma–inducible protein 16
0.5	R19956	VEGF	Vascular endothelial growth factor
Signal transduction			
0.09	W05628	PSHL	Phosphoserine phosphatase–like
0.09	W07300	AP1G1	Adaptor-related protein complex 1, gamma 1
0.25	N63635	P1M1	*Pim-1* protooncogene gene
0.25	AA598496	IQGAP	IQ motif containing GTPase-activating protein 1
0.25	AA019996	PTGER4	Prostaglandin E receptor 4 (subtype EP4)
0.25	AA397813	CKS2	CDC28 protein kinase regulatory subunit 2
0.25	AA446290	ST5	Suppression of tumorigenicity 5
0.25	AA489246	ST14	Suppression of tumorigenicity 14
0.25	N53172	RDCl	G protein–coupled receptor
0.33	AA443506	ARHGAP1	Rho GTPase–activating protein 1
0.33	H62028	DYRK3	Dual-specificity tyrosine (Y) phosphorylation-regulated kinase 3
0.33	AA453774	RGS16	Regulator of G-protein signalling 16
0.33	AA487560	CAV1	Caveolin 1, caveolae protein, 22 kDa
0.33	AA478542	AKAP12	AKAP12 A kinase (PRKA) anchor protein (gravin) 12
0.5	AA029737	TK2	Thymidine kinase 2, mitochondrial
0.5	AA496785	ABL1	Abelson murine leukemia viral oncogene homolog 1
Cytoskeleton			
0.09	AA521431	PFN1	Profilin 1
0.2	R22977	MSN	Moesin
0.25	AA490267	PLEK	Plekstrin
0.33	AA486942	CAPG	Capping protein (actin filament), gelsolin-like
0.33	AA411440	VIL2	Villin (ezrin)
0.4	AA069414	GFAP	Glial fibrillary acidic protein
0.5	AA487812	VIM	Vimentin
Apoptosis			
0.33	AA668595	PIG3	p53-induced gene 3
0.33	AA228130	PSIP2	PC4- and SFRSI-interacting protein 2
0.37	H45000	CASP4	Caspase 4
Transcription			
0.08	AA280677	ZNF258	Zinc finger protein 258
0.33	AA402207	EYA2	Eyes absent (*Drosophila*) homolog 2
0.33	N94468	JUNB	*Jun B* protooncogene
0.33	H26183	CEBPB	CCAAT/enhancer–binding protein (C/EBP), beta
0.5	P18146	EGR1	Early growth response 1
Proliferation			
0.33	AA454572	MCM2	MCM2 minichromosome maintenance–deficient 2, mitotin
Unknown function			
0.045	H93118	H93118	Hypothetical protein FLJ12592
0.04	R76499	R76499	Hypothetical protein BCOO7384
0.11	N29376	MNDA	Myeloid cell nuclear differentiation antigen
0.12	R78516	SELT	Selenoprotein T
0.14	AA481758	DNAJBl	DnaJ (Hsp40) homolog, subfamily B, member 1
0.2	AA490991	HNRPF	Heterogeneous nuclear ribonucleoprotein F
0.2	N8Ol29	MTIL	Metallothionein 1L
0.2	R64251	DDX38	DEAD/H (Asp-Glu-Ala-Asp/His) box polypeptide 38
0.25	AA486518	CLIC1	Chloride intracellular channel 1
0.33	N49629	UBD	Ubiquitin D
0.33	AA459318	TPD52	TPD52 tumor protein D52

I/C = average cDNA microarray ratios of invasive cells over tumor core cells.

transcriptionally upregulated in invasive glioma [11], points to potential interrelationships between motility and apoptosis resistance.

We propose that there is an invasion-specific gene expression profile—one that enables GBM cells to move through the brain parenchyma, creating two distinct subpopulations: the stationary, proliferative tumor core and the motile, invading tumor rim cells. Their distinct gene expression profiles suggest novel therapeutic targets that address dispersed, infiltrating tumor cells. This introduces the possibility of multiagent treatment modalities, specifically targeting invasive cells in conjunction with classic treatments aimed at the proliferating tumor core cells.

Materials and Methods

Clinical Samples and Histology

Human glioblastoma tumor samples were obtained from patients who underwent primary therapeutic subtotal or total tumor resection performed under image guidance. All specimens (13 in number) were collected and submitted to the study under institutional review board–approved protocols. None of the patients had been subjected to chemotherapy or radiotherapy prior to resection. The samples, which were obtained from the main tumor mass and the invasive edge, were immediately frozen on dry ice to be used in laser

capture microdissection (LCM). Another portion was fixed in paraformaldehyde and paraffin-embedded for histologic evaluation. Histologic diagnosis was made by standard light microscopic evaluation of hematoxylin and eosin–stained sections. All tumor samples were classified as WHO grade IV GBM [12].

LCM

LCM was performed as described previously [13]. Briefly, 1000 to 2000 tumor core and invasive cells were dissected from 8-μm sections cut from four flash-frozen glioblastoma (WHO grade IV) tumors. Cells in the tumor core were identified and captured; tumor cells immediately adjacent to necrotic areas; cortical areas; cells with small, regular nuclei; and endothelial and blood cells were avoided. White matter–invading GBM cells were identified by means of their nuclear atypia and heteropyknotic staining, which was consistent with that of the cells within the tumor core. Reactive astrocytes were discriminated through their distinct stellate morphology with eosinophilic cytoplasm and large, acentric, round nuclei, and were avoided.

RNA Isolation and Amplification

Total RNA was isolated from 1000 to 2000 LCM cells using the PicoPure RNA Isolation Kit (Arcturus, Mountain View, CA), and quantified by real-time reverse transcription polymerase chain reaction (RT-PCR) performed with the LightCycler (Roche, Mannheim, Germany). This consisted of performing PCR with Histone 3B primers using a serial dilution of cDNA of known concentration as a standard. The remaining RNA (approximately 10 ng) was amplified in two rounds with the RiboAmp RNA Amplification kit (Arcturus), yielding between 30 and 60 μg of copy RNA. RNA from one sample of very diffusely invaded white matter was also isolated (after microscopic inspection) and amplified to address the possible contribution of genetic material admixed from normal brain surrounding the captured invading cells.

cDNA Microarray Analysis

Six micrograms of amplified RNA was labeled in a RT in the presence of dUTP Cy3 (Amersham, Piscataway, NJ) utilizing random hexamers as primers. Universal reference RNA (Stratagene, La Jolla, CA) was amplified for one round in the same manner and labeled with Cy5 dUTP (Amersham). Labeled cDNA was hybridized overnight to 5750 gene cDNA microarray slides (Arizona Cancer Center, Tucson, AZ). (The complete gene list can be found in Supplementary Figure 1.) Following hybridization, slides were washed, scanned, and quantitated with the Axon GenePix 4000 microarray reader (Axon Instruments, Foster City, CA). Gene expression results were analyzed using GeneSpring (Silicon Genetics, Redwood City, CA) software. The measured intensity of each gene was divided by its reference channel (signal from the universal reference RNA) in each sample. When the fluorescence intensity of the reference channel was below 10, the data point was considered uninformative. Intensity-dependent normalization was also

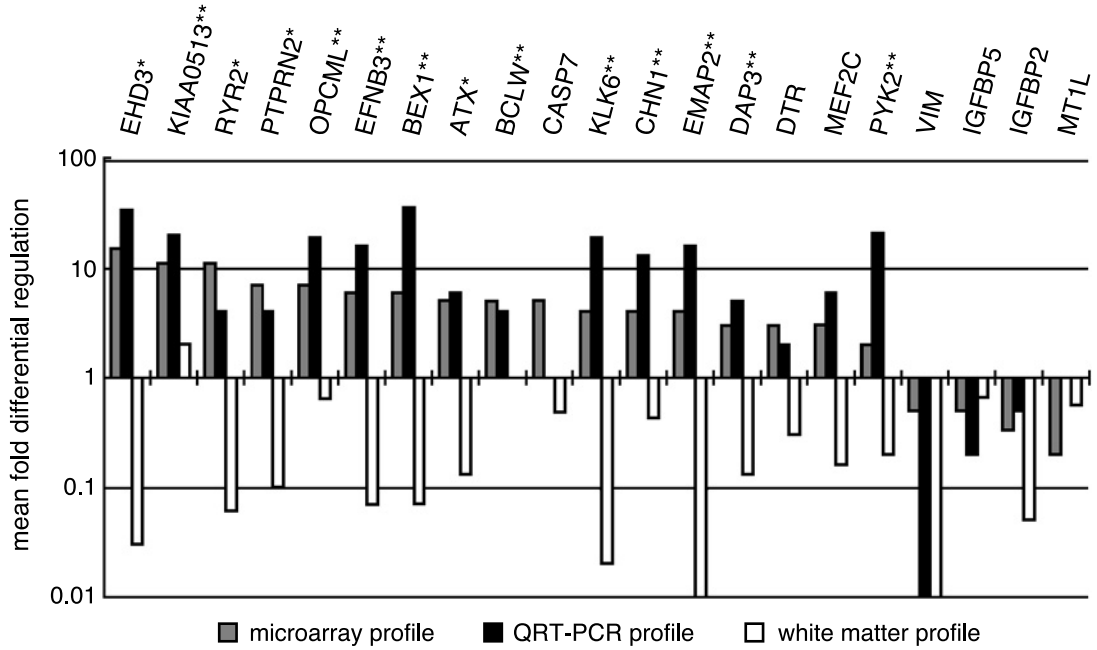

Figure 1. *QRT-PCR validation of gene candidates differentially expressed between invasive rim cells and tumor core cells in cDNA microarray analysis. Names of transcripts analyzed are on the x-axis and the mean fold differential regulation (difference in relative copy number, where 1 represents equal expression in both populations) is on the y-axis. Grey bars represent the mean gene expression levels of invasive tumor cells over tumor core cells seen in the cDNA microarray analysis. Black bars represent the mean gene expression levels of invasive tumor cells over tumor core cells as evaluated by QRT-PCR using seven matched tumor samples. White bars indicate the levels of gene expression (evaluated by QRT-PCR) in the diffusely invaded white matter from one of the samples used in the cDNA microarray analysis divided by the expression levels from either invasive cells (left side, where candidates genes are upregulated) or tumor core cells (right side, where candidate genes are downregulated) of the same sample. *Denotes genes with a significance of $P \leq .05$. **Denotes genes with a differential expression that reaches a significance of $P \leq .025$ as calculated using the Wilcoxon signed-rank test.*

applied, where the ratio was reduced to the residual Lowess fit of the intensity *versus* ratio curve. A fold change analysis was performed to identify differentially expressed genes. The ratios (sample over reference) for the three tumor core experiments and four invasive rim experiments were averaged and compared. Genes that were more than two-fold upregulated or downregulated were selected. Next, to address potential bias due to outliers, the gene lists were further screened by verifying that the same rim/core trend was present across samples that had matched core and rim populations. Genes following the trend in two of the three matched core/invasive rim sets were selected and tabulated. Complete lists of differentially expressed genes can be found in Supplementary Figure 2.

Quantitative RT-PCR (QRT-PCR) Validation

Total RNA was isolated from 500 to 1000 microdissected tumor core and invasive rim cells from 11 additional tumor samples as above. Seven samples were used to transcriptionally validate each gene candidate. Tumor RNA and RNA derived from the white matter adjacent to one of the tumor samples were reverse-transcribed with oligo dT primers using SuperScriptII (Invitrogen, Carlsbad, CA). The resulting cDNA was amplified by PCR with gene-specific primers (the list of primer sequences is available in online Supplementary Figure 3) (Operon/Qiagen, Alameda, CA) using the LightCycler and FastStart DNA Master SYBR Green I reagent (Roche). Log-linearity of the amplification curve for each primer set was confirmed down to the picogram range of cDNA. Specificity of PCR products was confirmed by melting curve analysis [14] and agarose gel electrophoresis. PCR protocols are disclosed in online Supplementary Figure 3. Quantification was done using Fit Points method of the LightCycler software version 3.5 [14]. The cDNA amount in each sample was normalized to the crossing point of the housekeeping gene *Histone 3B*. Relative mRNA fold upregulation in the invasive cells for each gene was calculated using the respective crossing points applied in the following

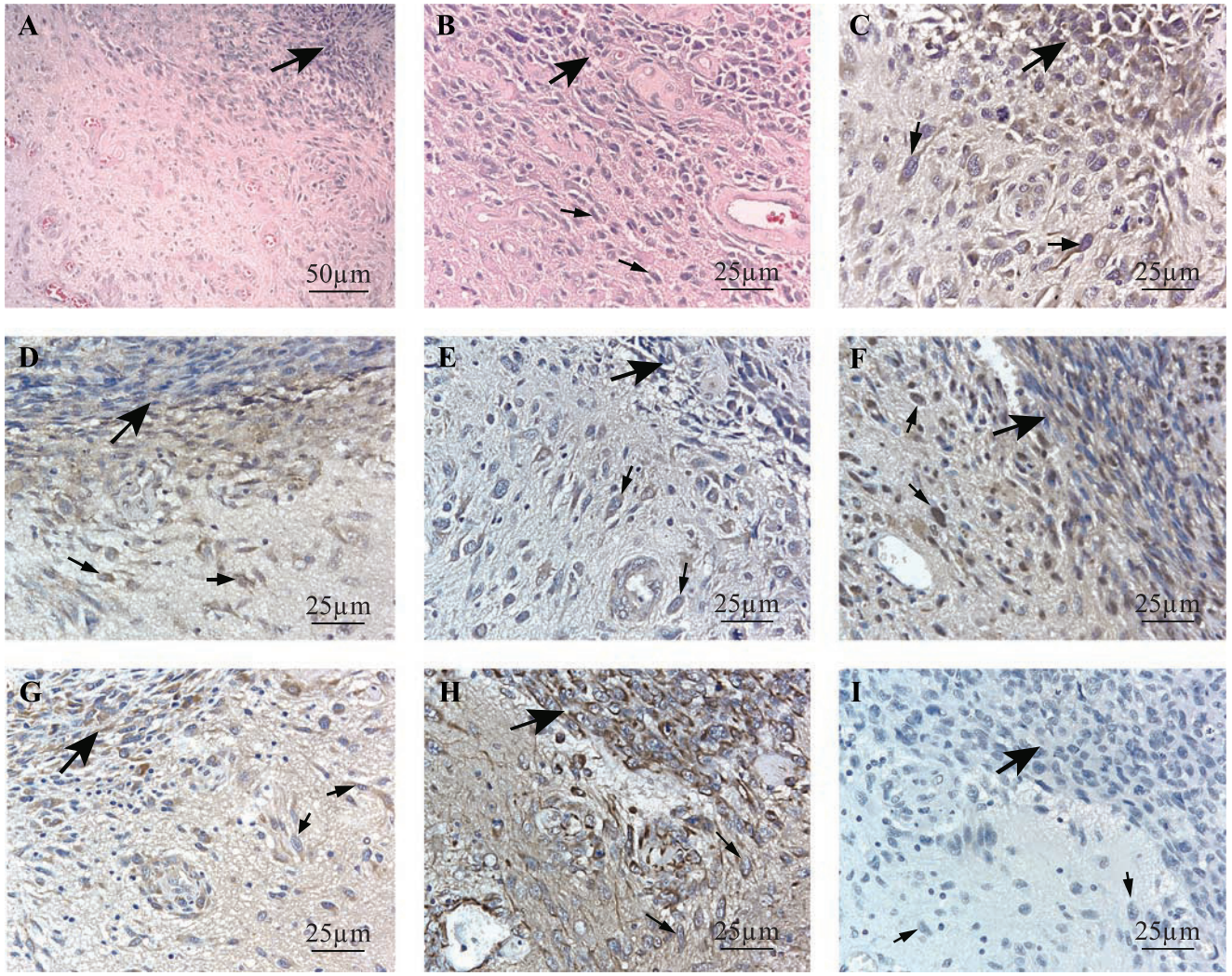

Figure 2. *Immunohistochemical analysis of six candidate genes ATX (C), BCLW (D), EFNB3 (E), PYK2 (F), IGFBP2 (G), and VIM (H); four overexpressed in the invasive rim cells and validated by QRT-PCR; and two underexpressed in the rim, respectively. (A and B) H&E stains of the glioblastoma invasion front. (I) Representative negative control. Large bold arrows point to the tumor core, and smaller arrows point at individually invasive glioblastoma cells. Original magnification, ×400, except (A) at ×200.*

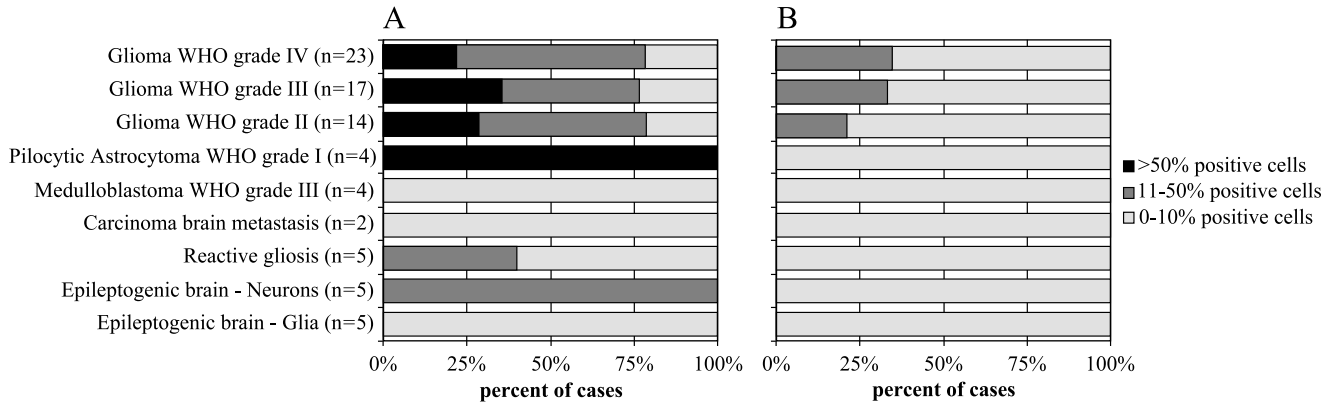

Figure 3. *Summary of immunohistochemical evaluation of ATX and BCLW in a glioma invasion tissue microarray. The tissue type examined and the number of samples in each category are listed on the y-axis. The percentage of cases with positively staining cells within each category is on the x-axis. The shading scale represents the percentage of positively stained cells within a sample. ATX TMA (A) evaluation showing a high degree of positive cells in gliomas of different grades, but also in some neurons and reactive astrocytes. The TMA stained for BCLW (B) reveals its presence in gliomas of all grades.*

formula: $F = 2^{(IH-IG)-(CH-CG)}$ (adapted from Ref. [15]), where F = fold difference, C = core cells, I = invasive rim cells, G = gene of interest, and H = housekeeping (*Histone 3B*). Statistical significance of the differential gene regulation was assessed using the Wilcoxon signed-rank test.

Immunohistochemical Confirmation of Gene Candidates

The protein products of six gene candidates validated by QRT-PCR were examined by immunohistochemistry on three GBM specimens. Briefly, 6-μm sections were heated for 2 hours at 65°C, deparaffinized in xylene and hydrated in a graded alcohol series, and subjected to antigen-specific epitope retrieval.

This was followed by quenching of endogenous peroxidase activity through incubation in 3% hydrogen peroxide in methanol. Slides were blocked with 10% normal serum in 0.1% Triton X-100 TBS and incubated overnight with the respective antibody at 4°C. Secondary antibodies appropriate to the primary antibody (Vectastain Kits; Vector Laboratories, Burlingame, CA) were added for 1 hour at room temperature, washed, and developed with DAB (Sigma, St. Louis, MO). The slides were counterstained with hematoxylin 2 (Richard-Allen Scientific, Kalamazoo, MI) prior to visualization. Antibody sources and epitope retrieval were as follows: for ATX, slides were microwaved in 10 mM sodium citrate, and antibody 100A (a generous gift from Dr. Tim Clair) was used at a 1:500 dilution. Slides stained for BCLW were digested for 30 minutes at 37°C in 0.5% pepsin in 0.01 N HCl, using a 1:25 dilution BCLW N-19 (Santa Cruz Biotechnology, Santa Cruz, CA). Treatment for EFNB3 included microwaving in 10 mM sodium citrate and a 1:100 concentration of EFNB3 antibody (R&D Systems, Minneapolis, MN). Slides for VIM were digested for 30 minutes at 37°C in 0.5% pepsin in 0.01 N HCl, followed by a 1:200 dilution of VIM 3B4 (DakoCytomation, Carpinteria, CA). Conditions for PYK2 pY402 (1:25; Biosource, Camarillo, CA) were as previously described [16], as were those for IGFBP2 sc-6001 (1:100; Santa Cruz Biotechnology) [17].

Tissue Microarray (TMA) Assembly

A specific glioma invasion TMA was assembled by Dr. D. H. Friedrich using patient-consented cases selected from a database of histologic reports. Gliomas of WHO grades I to IV ($n = 69$) and control cases ($n = 25$) including other tumors, reactive gliosis, and "normal" brain specimens from epilepsy surgery were included. Briefly, five equidistant microsamples (600 μm cross section) were punched out of donor paraffin blocks along a histologically verified invasion gradient and arrayed into the TMA using an arraying device (Beecham Instruments, Sun Prairie, WI) as described elsewhere [18]. The TMA paraffin block was then cut in 5-μm slices, which were tape-transferred and subjected to the described staining methods.

Results

Microarray Analysis of Laser Capture–Microdissected Glioma Cells Reveals Two Transcriptional Profiles

Using LCM, we collected two distinct GBM subpopulations based on their pathologic and anatomic context. cDNA gene expression profiling, followed by fold change analysis, resulted in a list of differentially expressed genes that are well documented in glioma biology. Among the genes expressed in the tumor core whose expression is downregulated in invasive GBM cells were *IGFBP-2* and *IGFBP-5* (Table 1). Several transcriptional regulators involved in growth control were expressed in the core, including *ZNF258*, *EYA2*, *EGR1*, and *JUNB*. Genes whose products are involved in signal transduction cascades such as *PSHL*, *PIM1*, *IQGAP*, *RDC1*, and *RGS16* were transcriptionally depressed in invasive cells, as were the cytoskeleton-related genes *PFN1*, *MSN*, *PLEK*, *VIM*, and *CAPG*. Angiogenesis-related *VCAM1* and *VEGF*, two genes well known in glioma biology, reflect the high degree of neovascularization of GBM. Heightened cellular proliferation, another definitive characteristic of GBM, is represented by *MCM2*. Interestingly, genes involved in drug resistance such as

Table 2. Genes Upregulated in Invasive GBM Cells.

I/C	Accession Number	Name	Description
Extracellular			
7	AA436142	SPOCK	Sparc/osteonectin, cwcv and kasal-like domains proteoglycan (testican)
6	AA425947	DKK3/RIG	Dickkopf (*Xenopus laevis*) homolog 3
6	AA115876	PI12	Serine (or cystein) proteinase inhibitor, clade 1 (neuroserpin) 1
4	R76614	NTN14	Netrin4
Transmembrane proteins			
69	H42679	HLA-DRA	Major histocompatibility complex, class II DM alpha
8	N62620	KCNK1	Potassium channel, subfamily K, member 1 (TWIK-1)
7	R38201	OPCML	Opioid-binding protein/cell adhesion molecule-like
7	AA464590	PTPRN2	Protein tyrosine phosphatase receptor type, N polypeptide 2
6	AA485795	EFNB3	Ephrin B3
6	H08933	GRIN2A	Glutamate receptor, ionotropic, *N*-methyl D-aspartate 2A
6	R40790	GABRG2	Gamma-aminobutyric acid (GABA) A receptor, gamma 2
5	T80232	ATX	Autotaxin (ectonucleotide pyrophosphatase/ phosphodiesterase 2)
5	AA417654	FGFR3	Fibroblast growth factor receptor 3
5	AA393408	PDE1A	Phosphodiesterase 1A, calmodulin-dependent
4	W48713	EGFR	Epidermal growth factor receptor
4	AA454743	KLK6	Kallikrein 6
4	N94270	TPARL	TPA-regulated locus
3	R17717	CDH13	Cadherin 13
3	H07878	GPRl9	G protein–coupled receptor 19
3	R14663	DTR	Diphtheria toxin receptor (heparin-binding EGF-like growth factor)
3	AA479243	AMFR	Autocrine motility factor receptor
Intracellular signaling			
23	H23046	RGS7	Regulator of G-protein signaling 7
15	R22326	EHD3	EH domain containing 3
11	R15791	RYR2	Ryanodine receptor 2 (cardiac)
10	AA064973	CS-1	Calcineurin-binding protein calsarcin-1
6	R69354	SAC2	Sac domain containing inositol phosphatase 2
4	AA464067	ITPK1	Inositol 1,3,4-triphosphate 5/6 kinase
3	AA449831	GRB2	Growth factor receptor–bound protein 2
3	AA454947	AKAP1	A kinase (PRKA) anchor protein 1
3	AA496013	STK2	Serine/threonine kinase 2
Cytoskeleton rearrangement			
59	AA448015	INA	Internexin, neuronal intermediate filament
4	R27680	EMAP2	Microtubule-associated protein like echinoderm EMAP
4	AA598668	CHN1	Chimerin (chimaerin) 1
3	H24688	SMARCC2	SWI/SNF–related, matrix-associated, actin dep reg of chromatin, C2
2	R85257	PYK2	Protein tyrosine kinase 2 beta
2	AA457036	P85SPR	PAK-interacting exchange factor beta (beta-pix)
Apoptosis			
5		BCL2L2	Bcl2-like 2 (Bcl-w)
5	T50828	CASP7	Caspase 7, apoptosis-related cysteine protease
3	R43325	DAP3	Death-associated protein 3
Transcription factors			
9	AA459941	PEG3	Paternally expressed 3
5	H60572	TRABID	TRAF-binding protein domain
4	N99243	TBX2	T-box 2
4	AA234897	MEF2C	MADS box transcription enhancer factor 2C
4	W00959	HLF	Hepatic leukemia factor
3	R42479	ETS2	V-ets E26 oncogene
Unknown function			
77	R67147	CRYM	Crystallin mu
16	H54364	MAST3	Microtubule associated serine/threonine kinase 3
11	H24428	KIAA0513	KIAA0513 gene product
8	AA452725	NUCB1	Nucleobindin 1
7	AA456008	AF1Q	ALL1-fused gene from chromosome 1q
7	W48780	NP25	Neuronal protein
6	W60581	BEX1	Brain expressed, X-linked 1
5	AA227594	MAL	Mal, T-cell differentiation protein
4	H19439	DSCR1L1	Down syndrome critical region gene 1–like 1
4	R59579	PGDS2	Prostaglandin D2 synthase (21 kDa, brain)
4	H66616	GLG1	Golgi apparatus protein 1
3	H22481	NPTX1	Neuronal pentraxin I
3	H45376	NELL2	Nel (chicken)–like 2
3	T84156	LNX	Multi-PDZ-domain–containing protein

I/C = average cDNA microarray ratios of invasive cells over tumor core cells.

ABCC3 (multidrug resistance protein 3, *MRP3*) and metallothioneins, which could play a role in intrinsic drug resistance in gliomas, are highly expressed in tumor core samples and downregulated in invasive cells. Finally, there was evidence of a three-fold lower level of proapoptotic *PIG3* (p53-induced gene 3) message in motile cells.

The transcriptome of invasive GBM cells illustrates their biologic distinctivenes from their cognate tumor cores. Gene candidates found to be upregulated two-fold or greater in invasive cells suggests that they are functionally distinct cells (Table 2). There was a preponderance of genes involved in adhesion (*OPCML* and *SPOCK*), extracellular signal transduction (*PTPRN2*, *DKK3*, *EFNB3*, *GRIN2A*, *FGFR3*, *EGFR*, *GPR19*, and *DTR*), and cytoskeletal rearrangement (*INA*, *EMAP2*, *CHN1*, and *PYK2*). The serine proteinase *KLK6* was the only extracellular matrix–degrading enzyme differentially expressed among the genes on the chip. We also observed genes involved in intracellular signal transduction (*RGS7*, *EHD3*, *CS1*, *ITPK1*, *GRB2*, and *STK2*), as well as a subset of genes linked to apoptosis (*CASP7*, *BCLW*, and *DAP3*). Some highly upregulated genes were difficult to classify, such as *ATX*, an extracellular protein involved in melanoma migration, and the intracellular calcium channel, *RYR2*. In conclusion, it was possible to transcriptionally differentiate cell populations from the same tumor that resides in different microenvironments.

Gene Candidate Validation by QRT-PCR

Gene candidates that discriminate invasive from tumor core cells were validated by real-time QRT-PCR using unamplified RNA (Figure 1). The genes chosen reflect various cellular processes that may be involved in the biology of the invasive phenotype, as well as some unknown, yet highly differentially expressed candidate genes. Candidates for validation were also chosen along the magnitude of the range of differential gene expression to validate the selection algorithm. Each gene's differential expression was assayed pairwise in corresponding tumor core and invasive rim from seven different tumor samples. To address possible contamination from surrounding normal brain tissues, RNA from a section of white matter surrounding one of the tumors was used to measure the expression of candidate genes in white matter. We found that 15 of 17 of the gene candidates were expressed 10-fold lower in the white matter compared to the invasive tumor. The Wilcoxon signed-rank test was used to analyze the statistical significance of the difference in gene expression between the tumor core and the invasive cell populations. Statistically significant changes in gene expression at the $P \leq .025$ level were seen with *KIAA0513*, *OPCML*, *EFNB3*, BCLW, KLK6, *CHN1*, *EMAP2*, DAP3, and *PYK2* transcripts. Significant change in gene expression at the $.025 < P < .05$ level was reached by an additional three transcripts, *EHD3*, *PTPRN2*, and *ATX*. *CASP7* was not increased in six of seven tumor pairs examined, and thus did not verify the cDNA microarray analysis. We also examined four gene candidates decreased in the invading GBM cells. *IGFBP2* and *VIM* transcript levels were greater than two-fold lower in the majority of tumors analyzed (four of seven and six of seven, respectively). *IGFBP5* and *MT1L* were only decreased in less than half of the seven tumors analyzed. The directionality of the expression of these four tumor core gene candidates did not reach statistical significance using the Wilcoxon test. Differential transcription of invasion gene candidates derived from microarray analysis was validated by QRT-PCR and showed that the invasion transcriptome was not significantly influenced by admixture of genetic material from the white matter context in which they were located.

Immunohistochemical Evaluation of Gene Candidates

Verification of protein product was undertaken in three GBM samples for IGFBP2, VIM, ATX, EFNB3, BCLW, and *PYK2* (Figure 2). The invasion gene candidates ATX and EFNB3 (Figure 2, *C* and *E*) are transmembrane proteins that displayed predominantly cytoplasmic staining in the invading cells, but also in the tumor core. BCLW was present in invasive cells (Figure 2*D*), as well as in vascular endothelium and, to a lesser degree, in reactive astrocytes (data not shown). The biologically active, phosphorylated form of PYK2 showed perinuclear localization in invasive glioma cells as well as in some tumor core cells (Figure 2*F*). The two candidates from the tumor core that were transcriptionally downregulated in the infiltrating cell population were visualized immunohistochemically in three GBM samples. IGFBP2 (Figure 2*G*) showed distinct cytoplasmic staining in the tumor core and somewhat lighter cytoplasmic staining in invading cells. Cytoplasmic staining for IGFBP2 was also visible, to a lesser extent, in astrocytes and reactive astrocytes present in the invaded white matter surrounding the tumor. The intermediate filament VIM (Figure 2*H*) was strongly present in the GBM tumor core, vascular endothelium, astrocytes, and reactive astrocytes, but was markedly reduced in invasive glioma cells. These data indicate that the protein product of the selected genes is produced in glioma cells.

TMA Analysis of ATX and BCLW

We further examined ATX and BCLW expression on an invasion TMA assembled to reflect the dispersion of infiltrative glioma of various grades and cellular origins (Figure 3). ATX is strongly expressed in glioblastoma cells and is also clearly expressed by WHO grade II and grade III gliomas. Interestingly, it is highly expressed in the four pilocytic astrocytomas (WHO grade I) examined. Positive staining is evident in normal vascular endothelium and, to a lesser extent, in tumor vasculature. Weaker expression is observed in reactive astrocytes and Nissl bodies of some neurons. It is weakly or not expressed by carcinoma metastasis and not expressed by normal astrocytes and oligodendrocytes (Figure 3*A*). Further analysis of 10 GBM cases revealed that of the invasive cells, 51% were ATX-positive, whereas only 30% of tumor core cells had ATX immunopositivity (data not shown). One such representative tumor is illustrated in Supplementary Figure 4. BCLW immunopositivity is weaker, but it is nonetheless detectable in glioma cells. Its expression mildly increases, with progressive malignancy grades reaching its peak in GBM (Figure 3*B*). As with ATX, no expression was seen in normal astrocytes and oligodendrocytes, nor was it present in metastatic adenocarcinoma or medulloblastoma. These data show that ATX and BCLW, two proteins not previously associated with glioma biology, are expressed in invasive glioma cells.

Discussion

Glioblastomas display a notoriously heterogeneous phenotypic presentation [19], yet there are key genetic changes that define these tumors [20]. Epidermal growth factor receptor (EGFR) overexpression/amplification occurs in primary GBM, which constitutes roughly 50% of gliomas. GBM that progresses from lower grades (secondary GBM) does not overexpress EGFR, but exhibits a loss of p53 [21]. These molecular subtypes of glioblastoma have distinct transcriptional profiles [22], which will be useful in targeting new therapies to a potentially more responsive subset of tumors. Previous gene expression profiles of glial tumors show that GBM can be differentiated from lower grades of astrocytic tumors through a characteristic group of upregulated genes [6]. Our studies reflect the expression of such GBM hallmark genes, which include *IGFBP2*, *IGFBP5*, *VEGF*, *VCAM1*, *EGFR*, *MCM2*, and *TNC* [4–6] in both tumor core and invasive cells. Interestingly, most of these genes are downregulated in the invasive cell population

relative to the tumor core. Expression of these genes in conjunction with the histopathologic diagnosis confirms the identity of the infiltrating cells as GBM cells. Analysis of the gene expression profile from the white matter surrounding one of the tumors indicates that the gene expression profile of invasive glioma cells is not attributable to contaminating mRNA from the white matter that they invade (Figure 1). Furthermore, glial fibrillary acidic protein (GFAP) is moderately transcriptionally downregulated in invasive glioma cells as compared to the tumor core population (Table 1). Immunohistochemical staining for GFAP further corroborates this finding (Supplemental Figure 5) and reveals that GFAP levels are much higher in normal and reactive astrocytes than in invasive tumor cells. Because GFAP levels are reduced with increasing astrocytic malignancy [23], it follows that the invasive transcriptome is not influenced by contribution of genetic material stemming from reactive astrocytes.

The importance of the tumor's microenvironment as a contributing factor to gene expression changes should not be overlooked [24]. Cells at the tumor core are densely packed, proliferative, and may experience considerable hypoxia leading to extensive areas of necrosis. Individually infiltrating cells interact with the extracellular matrix and diverse cells residing in the brain parenchyma, incorporating signals as they invade. Interactions with such diverse microenvironments likely contribute significantly to the initiation and maintenance of these discrete transcription profiles.

The expression profile of invasive glioma provides new insight into the interplay of the concerted molecular phenomena activated during invasion. Two such apparently linked mechanisms are motility and apoptosis resistance. Various types of cancer, such as glioma [11,25], gastric cancer [26], Kaposi's sarcoma [27], and pancreatic cancer [28], show evidence for this relationship. Recent evidence suggests that this occurs at the level of gene expression in breast cancer [29] and glioma [30], corroborating our findings that the invasion transcriptome shows a concomitant upregulation of genes involved in motility and apoptosis resistance.

Genes Involved in Motility-Related Pathways Are Differentially Regulated in Invasive Cells

Motility is dependent on cytoskeletal rearrangement and the extension of filopodia and then lamellipodia at the leading edge; these phenomena are modulated by Cdc42, Rac, and Rho [31]. The tight regulation of actin polymerization also emerges from this molecular portrait. Heightened expression of capping protein and profilin in the tumor core may inhibit filamentous actin polymerization and elongation, as overexpression of profilin in breast cancer reduces migration and invasion [32]. ERM (ezrin, radixin, and moesin) proteins, two of which are overexpressed in the core, act as linkers between the plasma membrane and the actin cytoskeleton, impairing migration-associated processes, such as cell spreading, attachment, and motility [33,34]. Involvement of small G-protein signaling and motility-related cytoskeleton rearrangement are illustrated by the differential expression of chimaerin alpha 1 (CHN1), a GTPase-activating protein for Cdc42 and Rac1 [35], which induces the formation of lamellipodia and filopodia in neuroblastoma cells [36]—key hallmarks of Cdc42 and Rac1 activation. Microinjection of full-length *CHN1* colocalizes with filamentous actin microspikes as well as with membrane ruffles, and is involved in the redistribution of focal adhesion protein vinculin. PYK2 is a member of the focal adhesion kinase family of nonreceptor tyrosine kinases; it is closely involved with src-induced increased actin polymerization at the fibroblastic cell periphery [37]. Its role in glioma migration/invasion is becoming clearer, as overexpression of PYK2 induced glioblastoma cell migration in culture [16]. Levels of activated PYK2 positively correlated with the migration phenotype in four glioblastoma cell lines (SF767, G112, T98G, and U118) tested in a two-dimensional migration assay [16]. Our analysis of activated PYK2 in GBM invasion *in situ* revealed strong staining in infiltrating GBM cells.

Tumor mitogens such as the cytokine ATX, which is an autocrine motility factor in melanoma [38] and breast cancer [39], as well as an autocrine motility factor receptor [40] and Netrin 4 [41], are also involved in promoting cell movement. A growing body of literature documents ATX's role in cancer invasion; we therefore chose to examine its expression in a glioma invasion–specific TMA. Evaluation of ATX staining revealed that it is expressed in all grades of glioma, but not in normal astrocytes. It also appears that almost twice the number of invasive tumor cells expresses ATX when compared to its expression in the tumor core. These findings suggest that the role of ATX in glioma invasion should be examined further.

Invasive Cells May Pre-empt Apoptosis

There is a positive correlation between apoptosis index (AI) and progressive grades of astrocytoma malignancy [42,43]. However, within GBM, there is a direct correlation between AI and patient survival, indicating that the most malignant GBM (measured by a shorter progression-free survival) has a lower rate of apoptosis [44]. It is of interest that the most malignant tumors are highly invasive [45]. Higher expression of antiapoptotic bcl-2 family proteins in recurrent GBM, even in patients who did not receive adjuvant chemotherapy or radiotherapy, points to the intrinsic resistance to apoptosis of these tumors [46]. We report BCLW (a member of this family), which is transcriptionally upregulated and expressed in invasive glioma cells. This finding reflects the previously observed expression of BCLW in infiltrative morphotypes of gastric cancer [47]. The mechanism by which BCLW acts in glioma cells is not known, but this family of apoptosis suppressors has been implicated in coordinating Ca^{2+} balance between the endoplasmic reticulum (ER) and mitochondria [48]. Recently, Ca^{2+} homeostasis has been linked to apoptosis [49], showing that Ca^{2+} release from the ER protects cells from apoptosis; interestingly, Ca^{2+} release is modulated, in part, by ryanodine receptors [50] and we found *RYR2* to be consistently upregulated in invasive glioma cells.

A direct correlation between invasion and apoptosis resistance can also be effected by modulation of apoptotic signaling. Such may be the case with DAP3, originally

described as a proapoptotic protein that transduces tumor necrosis factor ligand–dependent signals from death receptor DR4 through FADD (Fas-associated by death domain) [51] in fibrosarcoma cells. DAP3, however, was also described as an antiapoptotic factor in migrating glioma cells [11]. We propose that the equilibrium between proapoptotic and antiapoptotic proteins may be regulated, in part, by transcriptional activation of apoptosis modulators (such as DAP3) and antiapoptotic genes (such as *BCLW*) during activation of the invasive phenotype.

Current treatment for GBM includes surgical resection, chemotherapy, and radiotherapy, but despite continuous improvements in these approaches, patients' median survival remains at 1 year. New treatment modalities such as targeted therapy with monoclonal antibodies and immunotoxin-conjugated antibodies [52] are aimed at tyrosine kinase receptors such as EGFR and PDGFR, which are frequently overexpressed in glioblastomas. Gene therapy for GBM has met with some success in clinical trial [53], but is still in the early stages of development. Signaling pathways such as those involving EGFR, PDGFR, PI3K/AKT, and RAS can be targeted with small molecule inhibitors. However, most of these approaches predominantly address key pathways involved in cell proliferation, whereas recurrent tumors regrow from the cells that have invaded the brain and may be temporally less proliferative [54]. This preliminary study of glioma invasion–related gene regulation suggests targets that are potentially upregulated in gliomas regardless of their molecular etiology. Further transcriptional profiling of invasive GBM cells in more tumors with known EGFR and p53 status should clarify if this profile can be subcategorized according to current molecular classifications. An expanded approach including transcriptional profiling of diffusely infiltrating gliomas of lower grades may lead to insight into general biochemical mechanisms necessary for invasion.

In conclusion, we propose that the gene expression profile of invading glioma reveals a pattern unique to this discrete population of cells. These transcriptional differences point to reasons why invasive GBM cells are unlikely to respond to conventional therapies aimed at a proliferative and stationary tumor mass that has been the reference tissue for the molecular genetic analysis of this disease. Understanding the genetic basis of the invasive behavior may lead to novel combination therapies that not only address the tumor core, but also this distinct subpopulation of cells that have proven refractory to treatment. We anticipate that this will suggest novel intervention strategies through combined modification of apoptotic cascades, or potential use of small compounds targeting extracellular receptors expressed by invading glioma cells.

Acknowledgements

We thank the following people for their contribution to the success of this project: Alf Giese, MD, Wendy Elder, MD, and Kris Smith, MD, for contributing the samples that made this study possible; Nikolai G. Rainov, MD, DSc, Mitsutoshi Nakada, MD, PhD, and Tim D. Demuth, MD, for expert review and helpful discussion of the manuscript; David H. Friedrich, MD, for the assembly of the invasion TMA; Galen Hostetter, MD, for informative pathology discussions; Jeanne Razevich and Kathy Goehring for expert technical histologic assistance; and the staff at Arcturus for excellent technical assistance.

References

[1] Giese A, Bjerkvig R, Berens ME, and Westphal M (2003). Cost of migration: invasion of malignant gliomas and implications for treatment. *J Clin Oncol* **21,** 1624–1636.

[2] Burger PC, Dubois PJ, Schold SC Jr, Smith KR Jr, Odom GL, Crafts DC, and Giangaspero F (1983). Computerized tomographic and pathologic studies of the untreated, quiescent, and recurrent glioblastoma multiforme. *J Neurosurg* **58,** 159–169.

[3] Kleihues P, Louis DN, Scheithauer BW, Rorke LB, Reifenberger G, Burger PC, and Cavenee WK (2002). The WHO classification of tumors of the nervous system. *J Neuropathol Exp Neurol* **61,** 215–225 (discussion, 226–219).

[4] Sallinen SL, Sallinen PK, Haapasalo HK, Helin HJ, Helen PT, Schraml P, Kallioniemi OP, and Kononen J (2000). Identification of differentially expressed genes in human gliomas by DNA microarray and tissue chip techniques. *Cancer Res* **60,** 6617–6622.

[5] Ljubimova JY, Khazenzon NM, Chen Z, Neyman YI, Turner L, Riedinger MS, and Black KL (2001). Gene expression abnormalities in human glial tumors identified by gene array. *Int J Oncol* **18,** 287–295.

[6] Rickman DS, Bobek MP, Misek DE, Kuick R, Blaivas M, Kurnit DM, Taylor J, and Hanash SM (2001). Distinctive molecular profiles of high-grade and low-grade gliomas based on oligonucleotide microarray analysis. *Cancer Res* **61,** 6885–6891.

[7] Fuller GN, Hess KR, Rhee CH, Yung WK, Sawaya RA, Bruner JM, and Zhang W (2002). Molecular classification of human diffuse gliomas by multidimensional scaling analysis of gene expression profiles parallels morphology-based classification, correlates with survival, and reveals clinically-relevant novel glioma subsets. *Brain Pathol* **12,** 108–116.

[8] Kim S, Dougherty ER, Shmulevich L, Hess KR, Hamilton SR, Trent JM, Fuller GN, and Zhang W (2002). Identification of combination gene sets for glioma classification. *Mol Cancer Ther* **1,** 1229–1236.

[9] Fuller GN, Rhee CH, Hess KR, Caskey LS, Wang R, Bruner JM, Yung WK, and Zhang W (1999). Reactivation of insulin-like growth factor binding protein 2 expression in glioblastoma multiforme: a revelation by parallel gene expression profiling. *Cancer Res* **59,** 4228–4232.

[10] Nutt CL, Mani DR, Betensky RA, Tamayo P, Cairncross JG, Ladd C, Pohl U, Hartmann C, McLaughlin ME, Batchelor TT, et al. (2003). Gene expression–based classification of malignant gliomas correlates better with survival than histological classification. *Cancer Res* **63,** 1602–1607.

[11] Mariani L, Beaudry C, McDonough WS, Hoelzinger DB, Kaczmarek E, Ponce F, Coons SW, Giese A, Seiler RW, and Berens ME (2001). Death-associated protein 3 (Dap-3) is overexpressed in invasive glioblastoma cells *in vivo* and in glioma cell lines with induced motility phenotype *in vitro*. *Clin Cancer Res* **7,** 2480–2489.

[12] Kleihues P and Webster KC (2000). World Health Organization Classification of Tumors. Pathology and Genetics. Tumors of the Nervous System IARC Press, Lyon, France.

[13] Mariani L, McDonough WS, Hoelzinger DB, Beaudry C, Kaczmarek E, Coons SW, Giese A, Moghaddam M, Seiler RW, and Berens ME (2001). Identification and validation of *P311* as a glioblastoma invasion gene using laser capture microdissection. *Cancer Res* **61,** 4190–4196.

[14] Roche Molecular Biochemicals ME (2000). LightCycler Operator's Manual. Version 3.5. Roche Diagnostics GmbH, Mannheim D-68298, Germany.

[15] Ivanov AI, Pero RS, Scheck AC, and Romanovsky AA (2002). Prostaglandin E(2)–synthesizing enzymes in fever: differential transcriptional regulation. *Am J Physiol Regul Integr Comp Physiol* **283,** R1104–R1117.

[16] Lipinski CA, Tran NL, Bay C, Kloss J, McDonough WS, Beaudry C, Berens ME, and Loftus JC (2003). Differential role of proline-rich tyrosine kinase 2 and focal adhesion kinase in determining glioblastoma migration and proliferation. *Mol Cancer Res* **1,** 323–332.

[17] Zhang W, Wang H, Song SW, and Fuller GN (2002). Insulin-like growth factor binding protein 2: gene expression microarrays and the hypothesis-generation paradigm. *Brain Pathol* **12,** 87–94.

[18] Kononen J, Bubendorf L, Kallioniemi A, Barlund M, Schraml P, Leighton

S, Torhorst J, Mihatsch MJ, Sauter G, and Kallioniemi OP (1998). Tissue microarrays for high-throughput molecular profiling of tumor specimens. *Nat Med* **4,** 844–847.

[19] Paulus W and Peiffer J (1989). Intratumoral histologic heterogeneity of gliomas. A quantitative study. *Cancer* **64,** 442–447.

[20] Louis DN, Holland EC, and Cairncross JG (2001). Glioma classification: a molecular reappraisal. *Am J Pathol* **159,** 779–786.

[21] Maher EA, Furnari FB, Bachoo RM, Rowitch DH, Louis DN, Cavenee WK, and DePinho RA (2001). Malignant glioma: genetics and biology of a grave matter. *Genes Dev* **15,** 1311–1333.

[22] Mischel PS, Shai R, Shi T, Horvath S, Lu KV, Choe G, Seligson D, Kremen TJ, Palotie A, Liau LM, et al. (2003). Identification of molecular subtypes of glioblastoma by gene expression profiling. *Oncogene* **22,** 2361–2373.

[23] Rutka JT, Murakami M, Dirks PB, Hubbard SL, Becker LE, Fukuyama K, Jung S, Tsugu A, and Matsuzawa K (1997). Role of glial filaments in cells and tumors of glial origin: a review. *J Neurosurg* **87,** 420–430.

[24] Gladson CL (1999). The extracellular matrix of gliomas: modulation of cell function. *J Neuropathol Exp Neurol* **58,** 1029–1040.

[25] Joy AM, Beaudry CE, Tran NL, Ponce FA, Holz DR, Demuth T, and Berens ME (2003). Migrating glioma cells activate the PI3-K pathway and display decreased susceptibility to apoptosis. *J Cell Sci* **116,** 4409–4417.

[26] Yamaguchi H, Tanaka F, Sadanaga N, Ohta M, Inoue H, and Mori M (2003). Stimulation of CD40 inhibits Fas- or chemotherapy-mediated apoptosis and increases cell motility in human gastric carcinoma cells. *Int J Oncol* **23,** 1697–1702.

[27] Buttiglieri S, Deregibus MC, Bravo S, Cassoni P, Chiarle R, Bussolati B, and Camussi G (2004). Role of PAX2 on apoptosis resistance and pro-invasive phenotype of Kaposi's sarcoma cells. *J Biol Chem* **279,** 4136–4143.

[28] Ishikawa S, Egami H, Kurizaki T, Akagi J, Tamori Y, Yoshida N, Tan X, Hayashi N, and Ogawa M (2003). Identification of genes related to invasion and metastasis in pancreatic cancer by cDNA representational difference analysis. *J Exp Clin Cancer Res* **22,** 299–306.

[29] Wang W, Wyckoff JB, Frohlich VC, Oleynikov Y, Huttelmaier S, Zavadil J, Cermak L, Bottinger EP, Singer RH, White JG, et al. (2002). Single cell behavior in metastatic primary mammary tumors correlated with gene expression patterns revealed by molecular profiling. *Cancer Res* **62,** 6278–6288.

[30] Giese A (2003). Glioma invasion—pattern of dissemination by mechanisms of invasion and surgical intervention, pattern of gene expression and its regulatory control by tumor-suppressor p53 and proto-oncogene *ETS-1*. *Acta Neurochir Suppl* **88,** 153–162.

[31] Maidment SL (1997). The cytoskeleton and brain tumour cell migration. *Anticancer Res* **17,** 4145–4149.

[32] Roy P and Jacobson K (2004). Overexpression of profilin reduces the migration of invasive breast cancer cells. *Cell Motil Cytoskelet* **57,** 84–95.

[33] Speck O, Hughes SC, Noren NK, Kulikauskas RM, and Fehon RG (2003). Moesin functions antagonistically to the Rho pathway to maintain epithelial integrity. *Nature* **421,** 83–87.

[34] Wick W, Grimmel C, Wild-Bode C, Platten M, Arpin M, and Weller M (2001). Ezrin-dependent promotion of glioma cell clonogenicity, motility, and invasion mediated by BCL-2 and transforming growth factor-beta2. *J Neurosci* **21,** 3360–3368.

[35] Ahmed S, Lee J, Kozma R, Best A, Monfries C, and Lim L (1993). A novel functional target for tumor-promoting phorbol esters and lysophosphatidic acid. The p21rac-GTPase activating protein-chimaerin. *J Biol Chem* **268,** 10709–10712.

[36] Kozma R, Ahmed S, Best A, and Lim L (1996). The GTPase-activating protein n-chimaerin cooperates with Rac1 and Cdc42Hs to induce the formation of lamellipodia and filopodia. *Mol Cell Biol* **16,** 5069–5080.

[37] Wang Q, Xie Y, Du QS, Wu XJ, Feng X, Mei L, McDonald JM, and Xiong WC (2003). Regulation of the formation of osteoclastic actin rings by proline-rich tyrosine kinase 2 interacting with gelsolin. *J Cell Biol* **160,** 565–575.

[38] Stracke ML, Krutzsch HC, Unsworth EJ, Arestad A, Cioce V, Schiffmann E, and Liotta LA (1992). Identification, purification, and partial sequence analysis of autotaxin, a novel motility-stimulating protein. *J Biol Chem* **267,** 2524–2529.

[39] Yang SY, Lee J, Park CG, Kim S, Hong S, Chung HC, Min SK, Han JW, Lee HW, and Lee HY (2002). Expression of autotaxin (NPP-2) is closely linked to invasiveness of breast cancer cells. *Clin Exp Metastasis* **19,** 603–608.

[40] Timar J, Raso E, Dome B, Ladanyi A, Banfalvi T, Gilde K, and Raz A (2002). Expression and function of the AMF receptor by human melanoma in experimental and clinical systems. *Clin Exp Metastasis* **19,** 225–232.

[41] Kennedy TE (2000). Cellular mechanisms of netrin function: long-range and short-range actions. *Biochem Cell Biol* **78,** 569–575.

[42] Carroll RS, Zhang J, Chauncey BW, Chantziara K, Frosch MP, and Black PM (1997). Apoptosis in astrocytic neoplasms. *Acta Neurochir (Wien)* **139,** 845–850.

[43] Bogler O and Weller M (2002). Apoptosis in gliomas, and its role in their current and future treatment. *Front Biosci* **7,** e339–e353.

[44] Kuriyama H, Lamborn KR, O'Fallon JR, Iturria N, Sebo T, Schaefer PL, Scheithauer BW, Buckner JC, Kuriyama N, Jenkins RB, et al. (2002). Prognostic significance of an apoptotic index and apoptosis/proliferation ratio for patients with high-grade astrocytomas. *Neuro-Oncology* **4,** 179–186.

[45] Chicoine MR and Silbergeld DL (1995). The *in vitro* motility of human gliomas increases with increasing grade of malignancy. *Cancer* **75,** 2904–2909.

[46] Strik H, Deininger M, Streffer J, Grote E, Wickboldt J, Dichgans J, Weller M, and Meyermann R (1999). BCL-2 family protein expression in initial and recurrent glioblastomas: modulation by radiochemotherapy. *J Neurol Neurosurg Psychiatry* **67,** 763–768.

[47] Lee HW, Lee SS, Lee SJ, and Um HD (2003). Bcl-w is expressed in a majority of infiltrative gastric adenocarcinomas and suppresses the cancer cell death by blocking stress-activated protein kinase/c-Jun NH_2-terminal kinase activation. *Cancer Res* **63,** 1093–1100.

[48] Pinton P, Ferrari D, Rapizzi E, Di Virgilio F, Pozzan T, and Rizzuto R (2002). A role for calcium in Bcl-2 action? *Biochimie* **84,** 195–201.

[49] Scorrano L, Oakes SA, Opferman JT, Cheng EH, Sorcinelli MD, Pozzan T, and Korsmeyer SJ (2003). BAX and BAK regulation of endoplasmic reticulum Ca^{2+}: a control point for apoptosis. *Science* **300,** 135–139.

[50] Fill M and Copello JA (2002). Ryanodine receptor calcium release channels. *Physiol Rev* **82,** 893–922.

[51] Miyazaki T and Reed JC (2001). A GTP-binding adapter protein couples TRAIL receptors to apoptosis-inducing proteins. *Nat Immunol* **2,** 493–500.

[52] Mischel PS and Cloughesy TF (2003). Targeted molecular therapy of GBM. *Brain Pathol* **13,** 52–61.

[53] Rainov NG and Ren H (2003). Gene therapy for human malignant brain tumors. *Cancer J* **9,** 180–188.

[54] Giese A, Loo MA, Tran N, Haskett D, Coons SW, and Berens ME (1996). Dichotomy of astrocytoma migration and proliferation. *Int J Cancer* **67,** 275–282.